CMS Note 2000/044

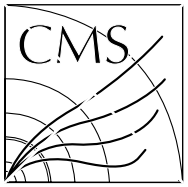

The Compact Muon Solenoid Experiment

CMS Note

Mailing address: CMS CERN, CH-1211 GENEVA 23, Switzerland

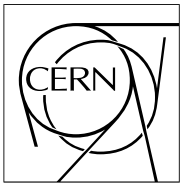

Current knowledge of BTI performance in magnetic field

J. Berdugo[1], M. Cerrada[1], N. Colino[1], M.C. Fouz[1], I. Lippi[2], R. Martinelli[2], L. Romero[1], L. Ventura[2], P.Zotto[3]

1. CIEMAT - Division de Fisica de Particulas, Madrid
2. Dipartimento di Fisica dell' Università di Padova and Sezione INFN di Padova
3. Dipartimento di Fisica del Politecnico di Milano and Sezione INFN di Padova

Abstract

The expected BTI performance in magnetic field was investigated using the software model developed for CMS simulation. The model was interfaced to data taken in the past years with DTBX prototypes. Efficiency and noise figures were obtained for all the available situations. Besides the effects of the most important filters available in the BTI operation flow were evaluated.

1 Introduction

The Bunch and Track Identifier (BTI) (shortly described afterwards) can be defined a straight line fitting device. The basic requirement for its correct operation is indeed that the points it is trying to connect belong to a straight line. The BTI is designed in order to be insensitive to deviations from linearity up to 12.5ns. In fact a lot of effort was put in the Barrel Muon Drift Chamber optics design to provide a controlled constant apparent drift velocity along the whole drift cell and this goal was undoubtedly reached for a large range of angle of incidence of the muons [1][2].

Problems arise with the increase of the particle incidence angle, since the actual active zone cannot of course be reduced below a few millimeters size, without causing severe inefficiencies. The performance of the BTI as a function of the incidence angle was already studied using prototype BTIs and important effects were found only for incident angles beyond 25° [3]. At larger angles the non-linearity was causing a rapid decrease of the probability of alignment of four hits and a contemporary increase of the fraction of three hits tracks: including both kinds of triggers the efficiency drop was negligible.

Another important variable in the CMS environment is the presence of a stray magnetic field. This is quite important in the corner regions close to the forward detector wheels. A magnetic field is adding to the electric field force ($e\vec{E}$) a magnetic field force ($e\vec{v} \times \vec{B}$) that is twirling the electron path to the anode. Unfortunately any significant test could not be performed using the BTI prototype until now, so in order to gain useful information its software model was interfaced to the collected data to provide useful information. In this way we skip the problem of correctly simulating the chamber response and past experience shows that in these conditions the model and the BTI performance agrees within few percent.

2 Short Description of BTI

The Bunch and Track Identifier was studied to work on each groups of four layers of staggered drift tubes called Super Layers (SL), aiming to the identification of the tracks giving a signal in at least three of the planes. We quickly recall the basic description of the device: any other detail can be found in Reference 3.

Each BTI is connected to nine wires allocated as shown in Figure 1.

The parameters computed from the BTI are the angular k-parameter k = h tan ψ (the track direction) and the crossing position, computed in the SL central plane. The geometrical quantities involved are shown in Figure 1: ψ is the angle of the track with respect to the normal to the chamber and h = 1.3mm is the distance between the wire planes.

These parameters are evaluated by means of a generalized mean-timer technique: this method is a search inside a BTI for the alignments of the recorded hits belonging to a track. If there is an alignment of four hits the signal is marked as High Quality Trigger (HTRG), while if it is due to the alignment of only three hits, it is marked as Low Quality Trigger (LTRG).

The alignment occurs with fixed delay with respect to the parent bunch crossing time, thus permitting its identification. The total latency of the BTI is determined by the maximum drift-time to the wires, TMAX, plus 4 clock cycles needed for input signal synchronization and BTI calculations. With the tested chamber the measured drift velocity is ~56 μm/ns and therefore the delay of the TRG signal with respect to the parent interaction is therefore 18 bunch crossings.

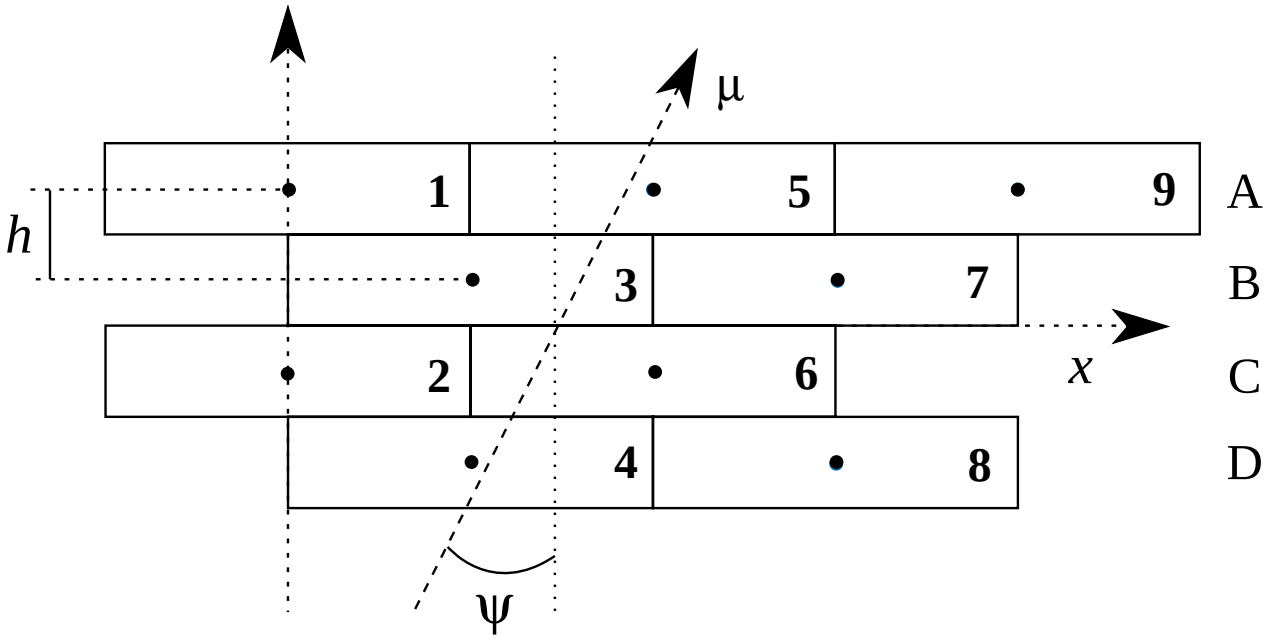

Figure 1- BTI layout showing channels allocation.

The BTI trigger algorithm actually generates HTRGs and LTRGs when the computed k-parameters of any of the predefined patterns of wires are equal within the programmed tolerance.

Position and angular resolution of the device depend on the drift velocity and on the sampling frequency of the device. In our case the angle is measured with a resolution better than 60mrad, while the position is measured with a resolution of 1.4mm. The angular resolution is track pattern dependent and is generally worse for LTRGs.The maximum angular acceptance is nominally $\psi_{MAX} = \pm 55°$, but the efficiency drops very fast beyond 45°.

Each SL is equipped with one BTI every four wires and the BTIs are overlapped by five wires assuring that every track, with angle within the maximum acceptance range, is fully contained in at least one BTI.

Only one track per bunch crossing per BTI is generated.

3 Data samples and event selection

The data used were recorded in 1996 at H2 using the Madrid Superlayers prototypes[4]. The following configurations were taken at different magnetic field B and for various incidence angle θ:

- B = 0T; θ = 0°, 14°, 24°, 34°, 44° and 49°
- B = 0T, 0.2T, 0.4T, 0.6T and 0.8T; θ = 0°
- B = 0T, ±0.2T, ±0.4T and ±0.6T; θ = 14° and 24°
- B = 0T, 0.2T, 0.4T, 0.6T, 0.8T and 1.0T; θ = 0°, 14°, 24°, 34° and 40°

The magnetic field components are defined in Figure 2. In the second and third sample the field was parallel to the wires having only B_w component, while in the last sample there were superlayers either with the wires or with the electric field set at angle θ. Therefore we had data with components $B_w = B\cos\theta$ and $B_n = B\sin\theta$ or components $B_E = B\cos\theta$ and $B_n = B\sin\theta$.

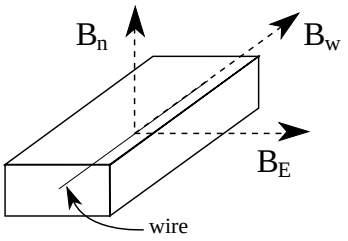

Figure 2- Definition of magnetic field components

Some of the detector wires were inefficient in the target zone and there was some unknown source of coherent noise: therefore it was not possible to analyze the available data without any selection bias. We had to process only events where at least one hit per layer was recorded and we used only the first hit recorded from the TDC after t_0. Hence we will quote only the probability of generating a trigger in the fully sensitive zone of the detector: despite being a limit to the analysis the applied cuts assures that the results will provide the actual BTI performance figures disembodying the chamber geometrical efficiency effects. These results will anyway retain the consequences connected to the electromagnetic background associated to the muon interaction with the chamber material.

4 BTI synchronization

Some setup parameters need to be determined in order to assure a correct operation of the BTI. The computation of these parameters was done using the zero field data only once in order to assure the direct comparison of the BTI figures for different magnetic field configurations. The first parameter is the maximum drift time (T_{MAX}) to the wire: this parameter is represented by a number with 12.5ns accuracy[1]. This is determined by the distribution of the mean-time of any three consecutive layers: the value obtained from Figure 3 is 356ns equivalent to ~28 clock steps. But the BTI works with time intervals and therefore it needs a calculation of the time origin. Actually this operation is the determination of the time difference between the BTI clock and the event trigger time as provided by the external scintillators setup. The actual determination provides a 1ns precision interpolation in the ±12.5ns window of the coarse T_{MAX} evaluation and is called BTI synchronization: the best phase between the BTI clock and the event time is determined from the data.

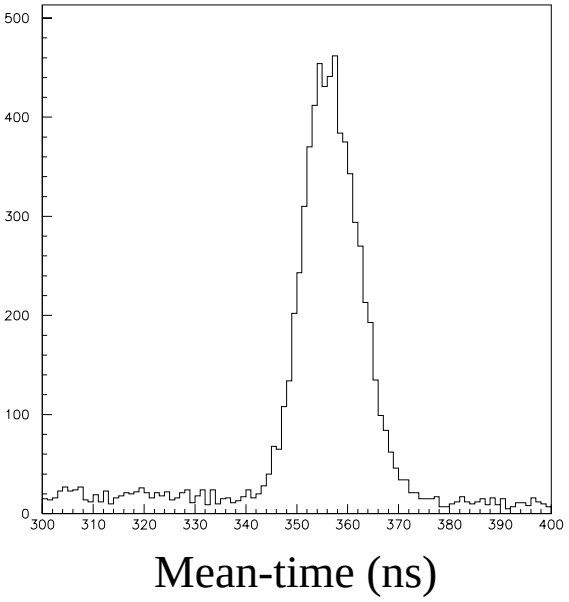

Figure 3- Mean-time at normal incidence.

The algorithm used to find the best value of the time delay is still based on a mean-timer operation. In self-triggering mode the drift times of each chamber are computed using the BTI

1. The actual BTI hardware device has a 6.25ns resolution.

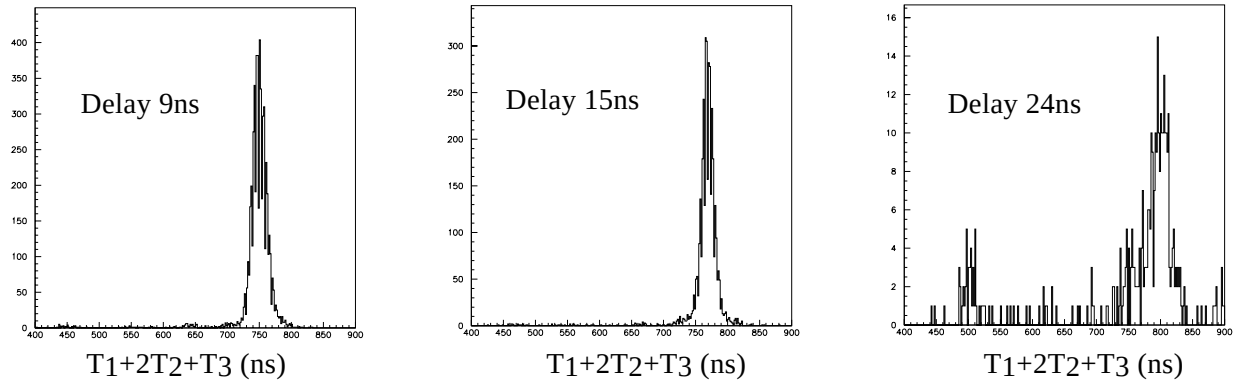

Figure 4- Distribution of the quantity T123 for the mixed incident angle sample.

trigger bunch crossing assignment. If the BTI phase is not correct there will be events assigned to the wrong bunch crossing. In this case the drift time will be calculated using an incorrect number and will be wrong by a LHC clock count. Computing the quantity $T_{123} = T_1+2T_2+T_3$ (1, 2, 3 are any three consecutive layers of the chamber) the events assigned to different nearby bunch crossings will be assigned to gaussian distributions of $\sigma \sim 8$ns whose centers will differ by about 100ns.The distribution of T_{123} for some delays at normal incidence is shown in Figure 4.

In order to reject events spoiled by δ-rays and have a clean distribution, T_{123} is required to be equal to T_{234} within 2σ. Moreover the BTI is programmed to its minimum tolerance for equation alignment and only HTRGs are accepted to maximize the separation between the peaks.

The indicator chosen to find the best time delay is the computation of the minimal root mean square of the T_{123} distribution, since its value does not depend on the trigger rate. The r.m.s. of the distribution is shown in Figure 5 for samples at 0°, 14°, 24° incident angle independently

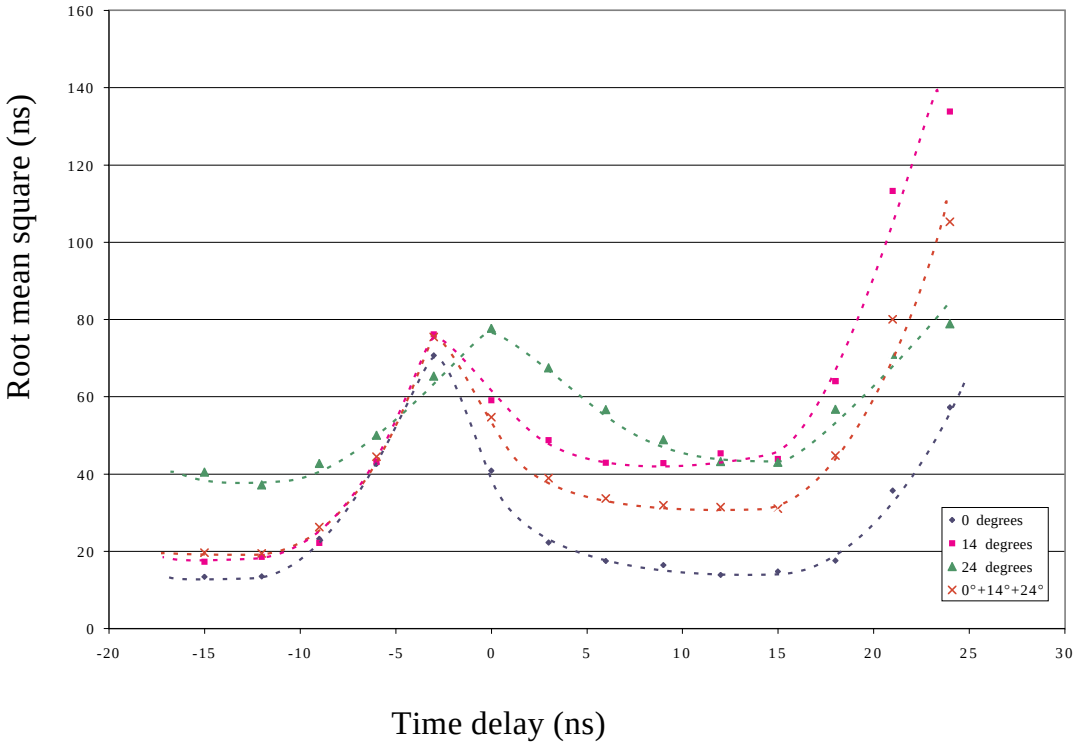

Figure 5- Root mean square of the quantity T123 as a function of the delay time. The function is periodic and the best choice for the delay time is the one corresponding to minimum r.m.s.

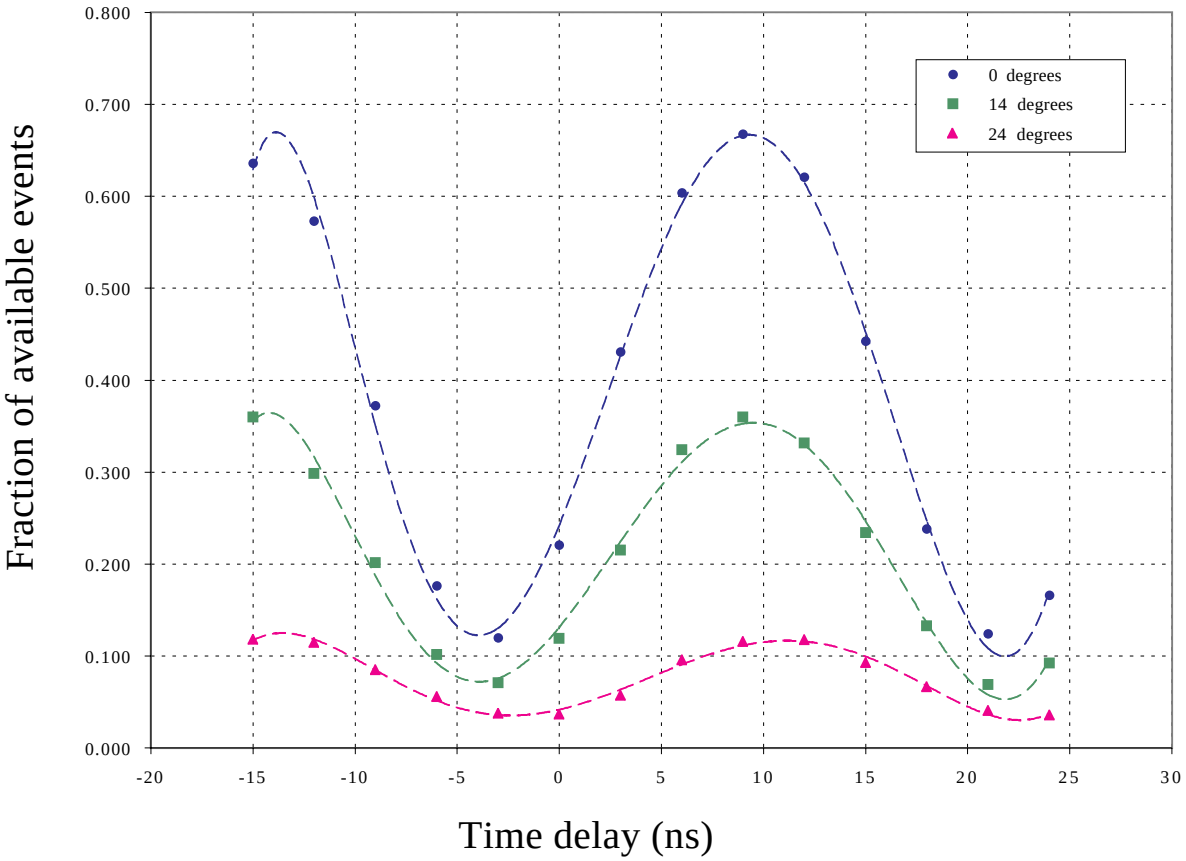

Figure 6- Probability for an event to pass the required cuts for BTI synchronization as a function of the time delay for different incidence angle

and for the global angle sample. The best phase slightly varies with the actual angle. Assuming that in CMS we will have a flat angular distribution, we use the value determined by the sample with various angles.

Figure 6 shows the probability for an event to survive the required cuts. It is evident that the fraction of usable events rapidly decreases with the incidence angle: indeed at ~27° the track will cross more than one cell per layer making impossible a clean event selection.

The time delay has a direct impact on the bunch crossing identification: as an example of the effect the time distribution of HTRGs is shown if Figure 7 for few time delays.

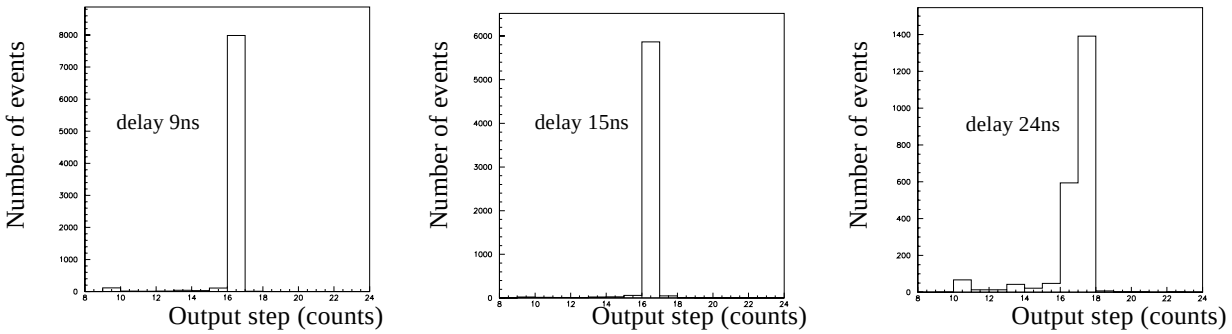

Figure 7- Bunch crossing assignment distribution of the events in the mixed sample for different time delays.

5 BTI performance

Once defined its basic parameters the BTI model was run on all the available data samples. The tests done on the BTI aimed to find the efficiency and the noise on zero field data and to evaluate the performance degradation expected in presence of magnetic field.

5.1 Performance without magnetic field

There are two basic ways to change the BTI performance.

The first one is the modification of the alignment tolerances. The BTI issues a HTRG at the coincidence of the six computed k-parameters: the coincidence occurs when these k-parameters are equal within an alignment tolerance that depends on the actual pair and equation considered. It is possible to force the tolerance to a fixed value of ±1 (minimal acceptance) or ±2 (maximal acceptance). Of course the minimal acceptance will reduce the fraction of HTRGs and the maximal acceptance will increase it.

The second one is the deactivation of a Low Trigger Suppression (LTS) filter, that is supposed to be active by default. The BTI is generating LTRGs at bunch crossings other than the correct one due to random alignments of only three k-parameters. The LTS mechanism cancels the LTRGs generated in a temporal window programmable in the range [-1bx,+8bx] around a HTRG. This kind of filter should be harmless, but the residual cell non-linearity is generating HTRGs at the bunch crossings nearby the right one, while issuing only a LTRG at the right bx. In this case the filter is unfortunately rejecting the good trigger and forwarding the wrong one.

The BTI efficiency with the LTS filter active and for the possible settings for the tolerance of BTI equations alignment is shown in Figure 8 as a function of the incidence angle. The standard choice does not differ substantially from the maximal tolerance, supporting the evidence of a correct choice for the standard values. Figure 9 and Figure 10 show how the fraction of HTRGs and LTRGs are changing for the selected tolerances on the same event sample.

While there are several filters acting on the LTRG noise all along the local drift tubes trigger chain, there is no similar filtering sequence for HTRGs. It is therefore really important to compute the HTRG noise level. The fraction of out of time HTRGs is shown in Figure 11.

The efficiency as a function of the incidence angle with the LTS filter on and off is shown in Figure 12: the activation of the filter causes a slight dependence of the efficiency on the angle, which is otherwise flat up to 45° as expected from the bench tests [5].

The residual non-linearity with the angle causes some HTRG wrong bunch crossing identification. The bunch crossing assignment quality is reported in Figure 13 for the analyzed data samples.

The BTI angular resolution can be extracted from the distribution of the BTI computed k-parameter reported Figure 14: each angle is clearly separated from the other ones, although it is clear that the resolution is somewhat worsening with increasing angle. It should be anyway reminded that the k-parameter is a function of $\tan\theta$ and therefore the angular acceptance is decreasing with increasing angle. It is not worth showing the impact position evaluation, since the wires' inefficiencies strongly bias the distribution.

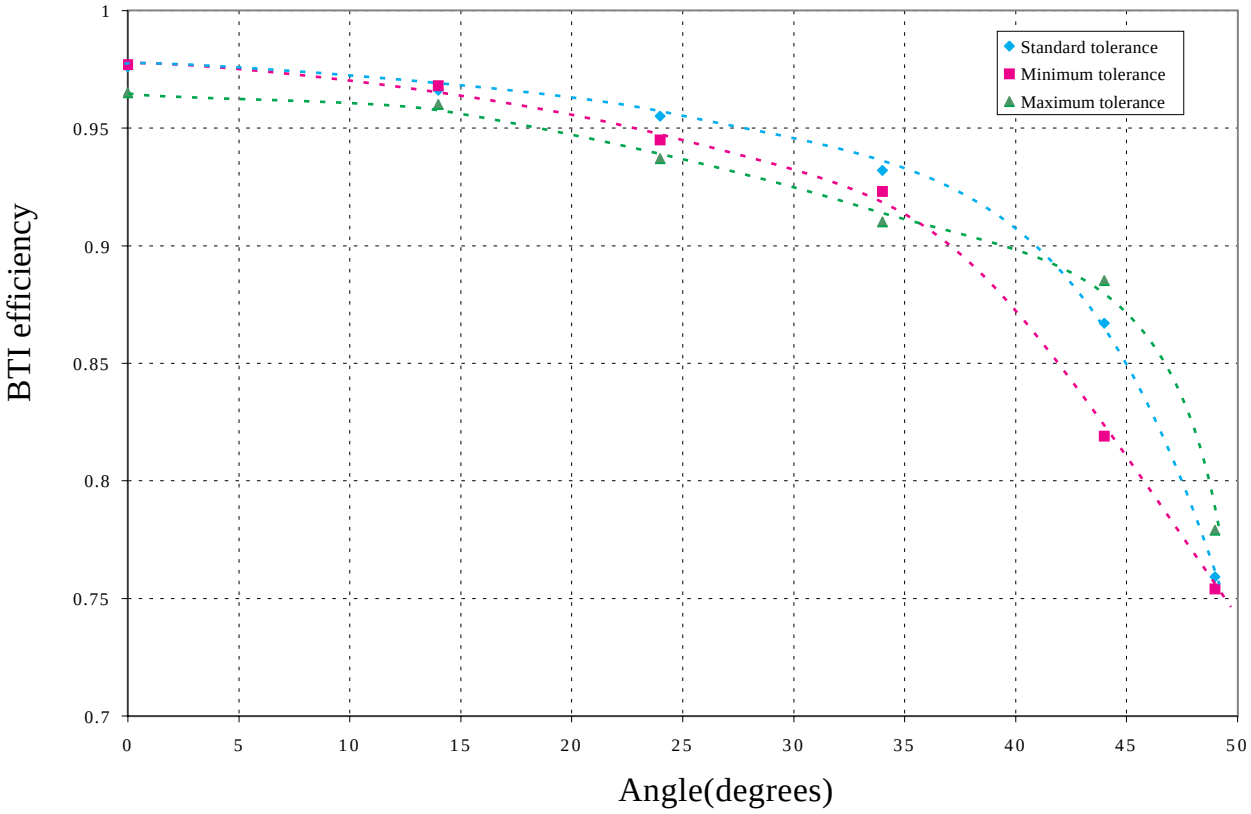

Figure 8- BTI efficiency versus incident angle for different alignment tolerances with LTS filter always active.

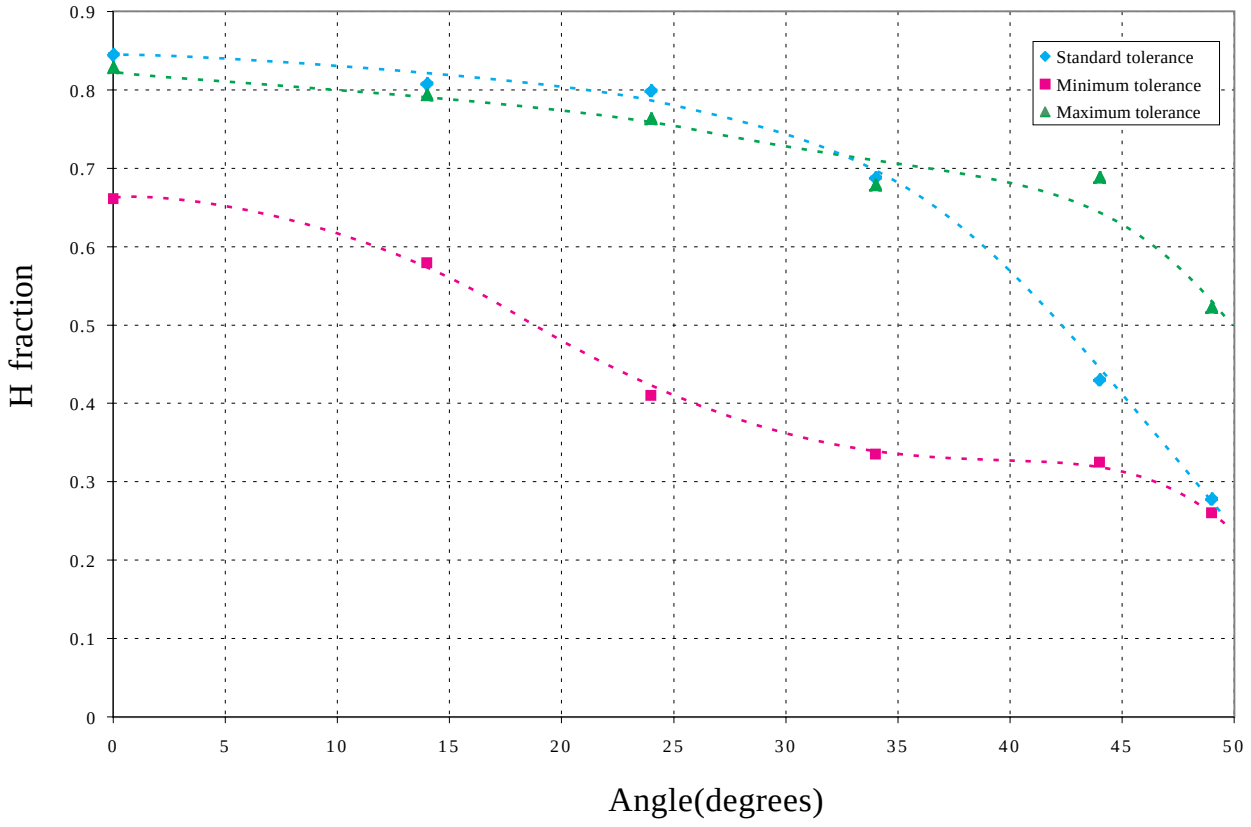

Figure 9- Fraction of HTRGs versus incident angle for different alignment tolerances with LTS filter always active.

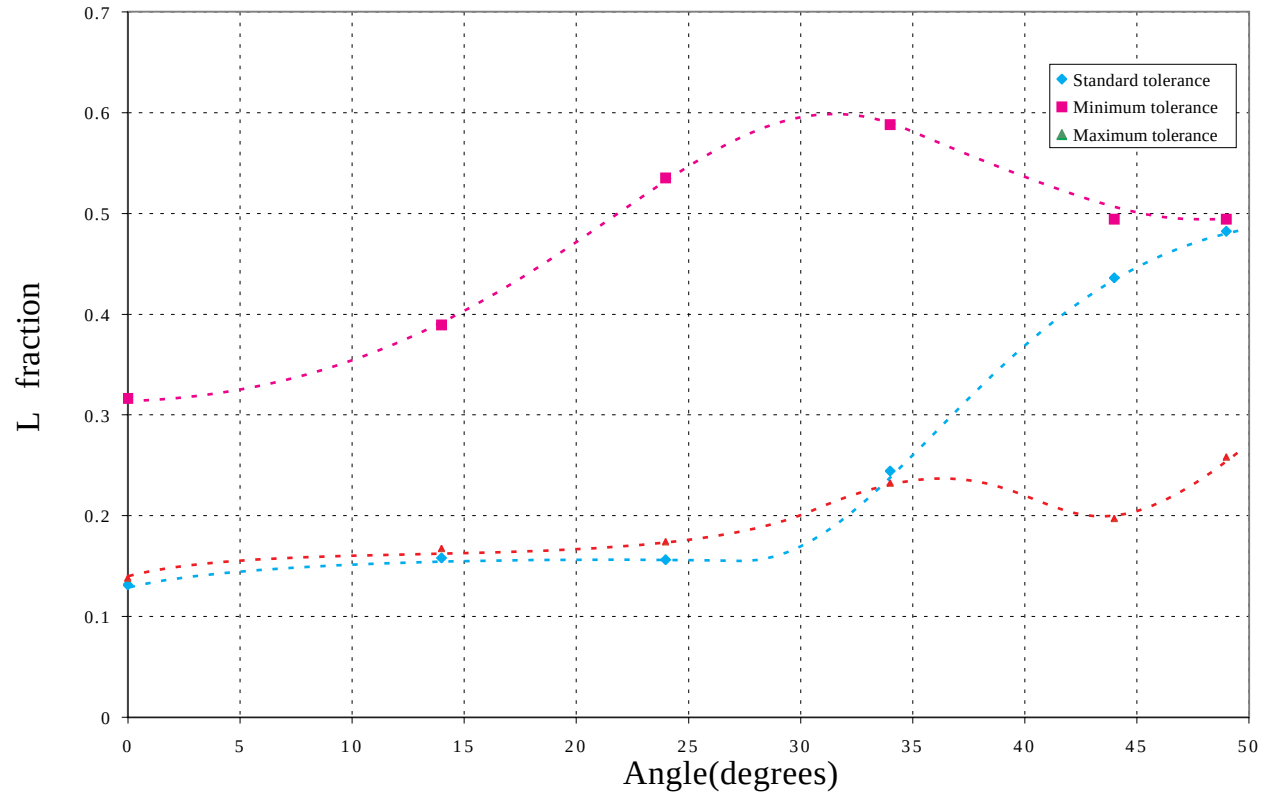

Figure 10- Fraction of LTRGs versus incident angle for different alignment tolerances with LTS filter always active.

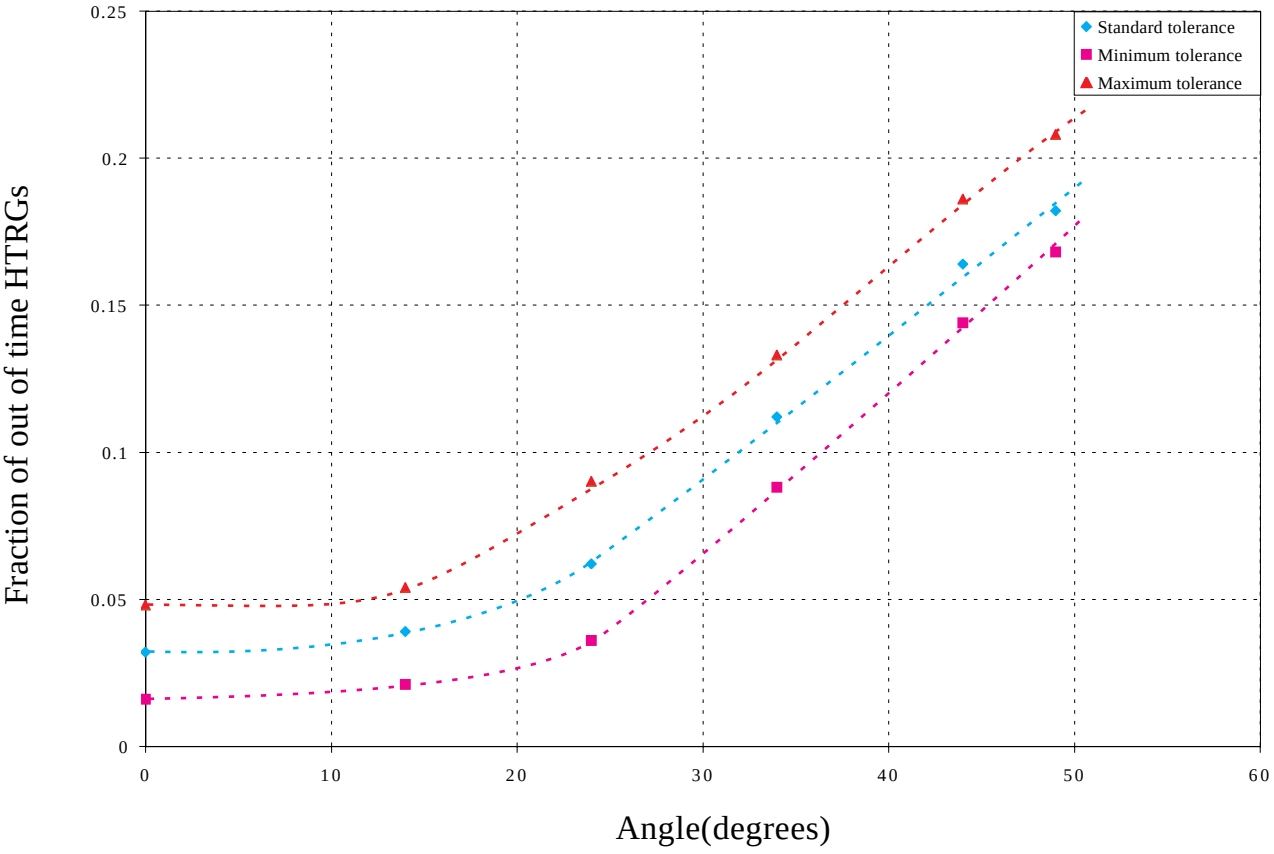

Figure 11- Fraction of HTRG noise versus incident angle for different alignment tolerances with LTS filter always active.

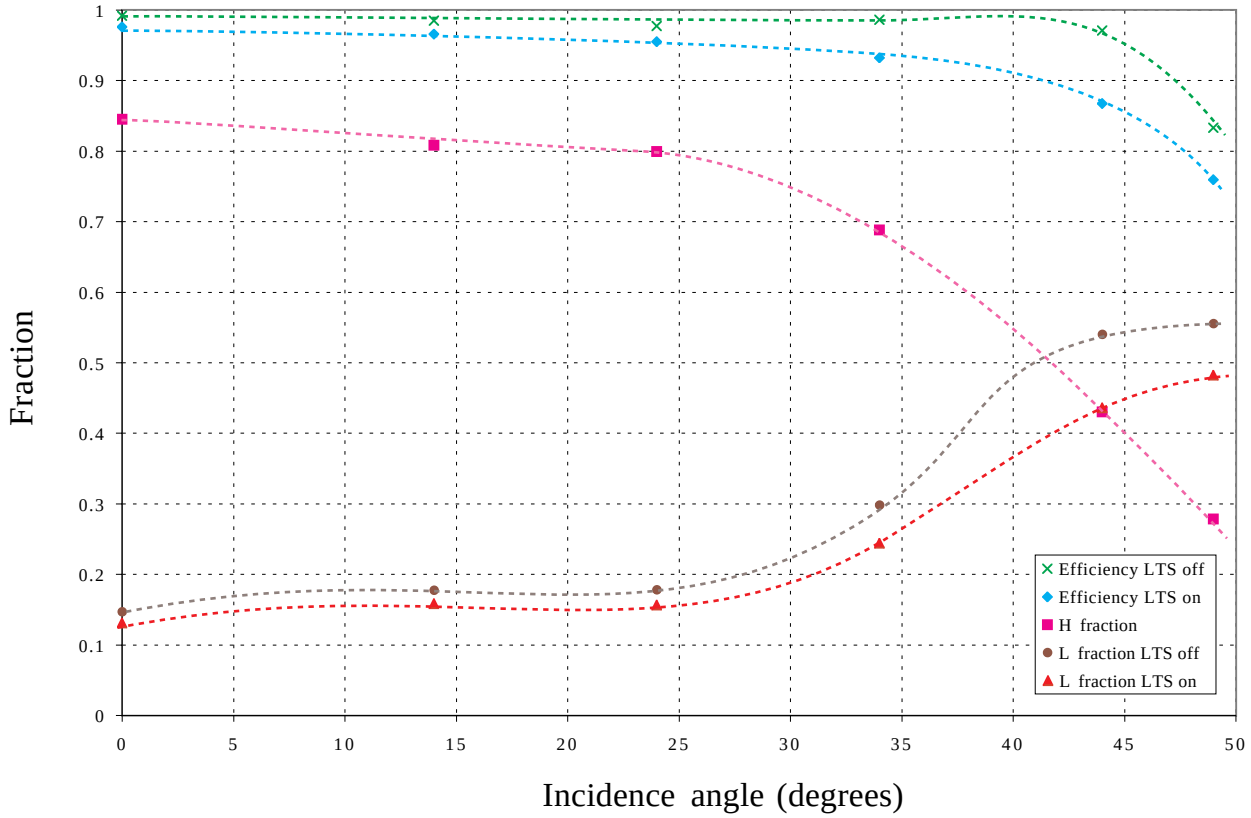

Figure 12- Comparison between efficiencies and fraction of HTRGs and LTRGs with and without the LTS filter.

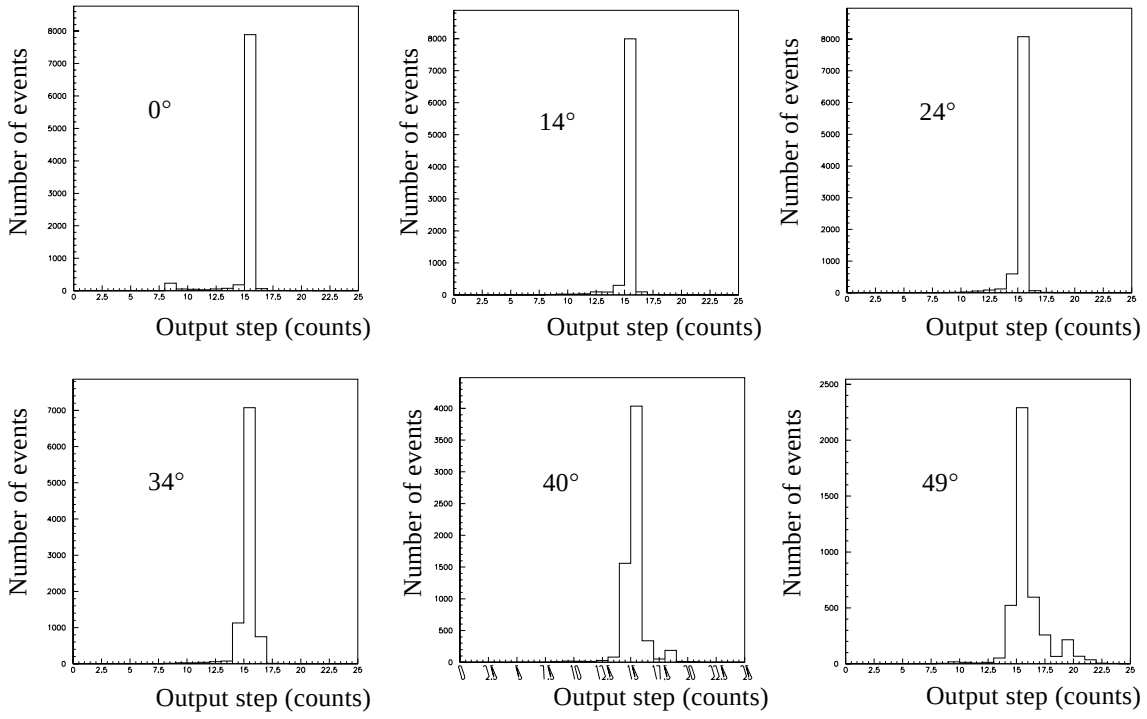

Figure 13- Bunch crossing assignment for HTRGs for different incidence angles

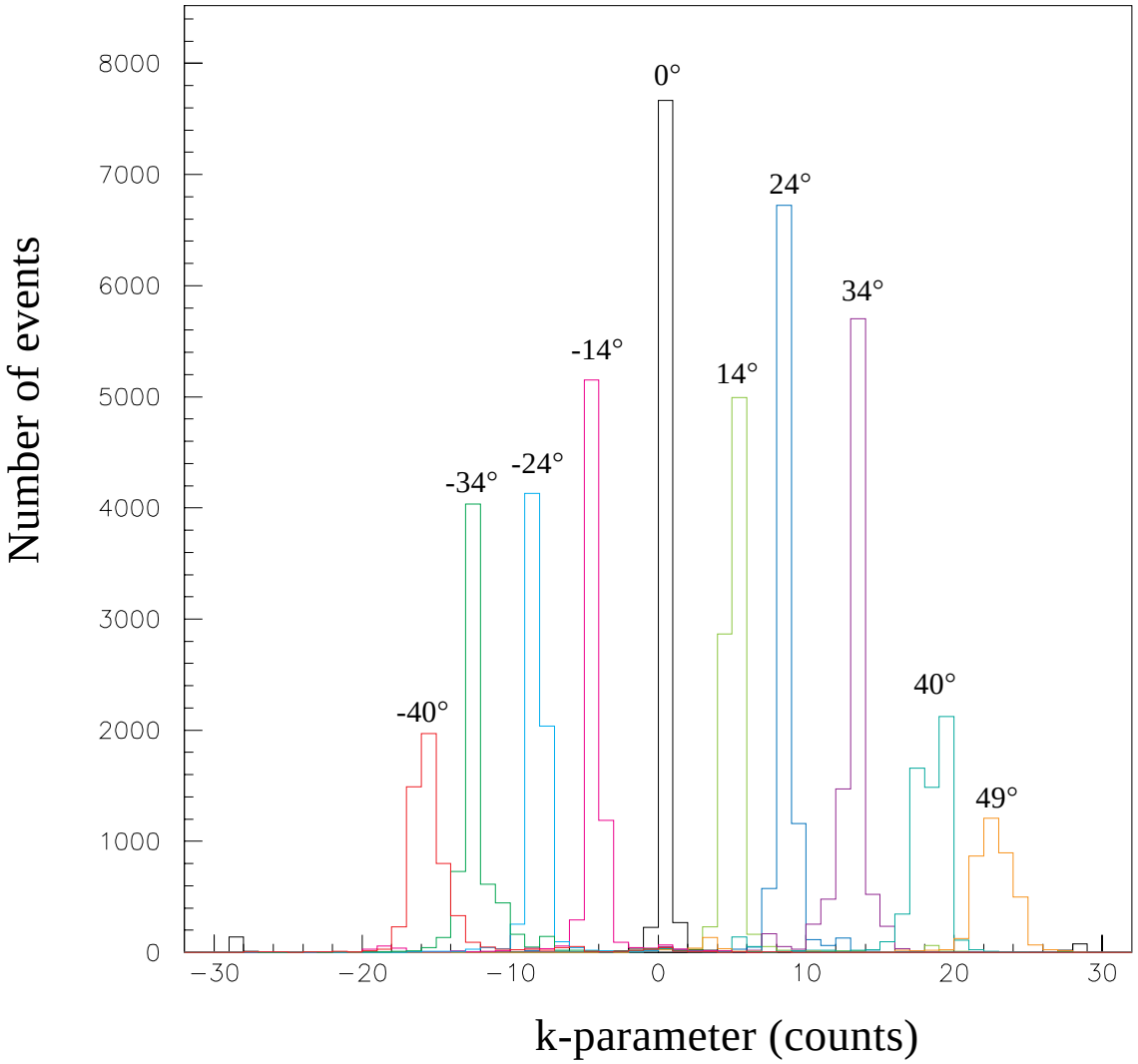

Figure 14- BTI k-parameter evaluation for different incident angles.

5.2 Performance with magnetic field

The BTI will be operating in a variable magnetic field region. The expected magnetic field map is shown in Figure 15. The radial component will be acting on all DTBX quadruplets, while the longitudinal component will correspond to B_w for the φ quadruplets and B_E for the θ quadruplets. In fact typical situations will be combinations of B_n < 1T and B_w or B_E < 02-04T components.

The available chamber rotations and relative field orientations allowed the study of the effects of

- pure B_w component at different incident angles
- pure B_E component at normal incidence
- mixed (B_n,B_E) with low B_n and high B_E
- mixed (B_n,B_w) with low B_n and high B_w

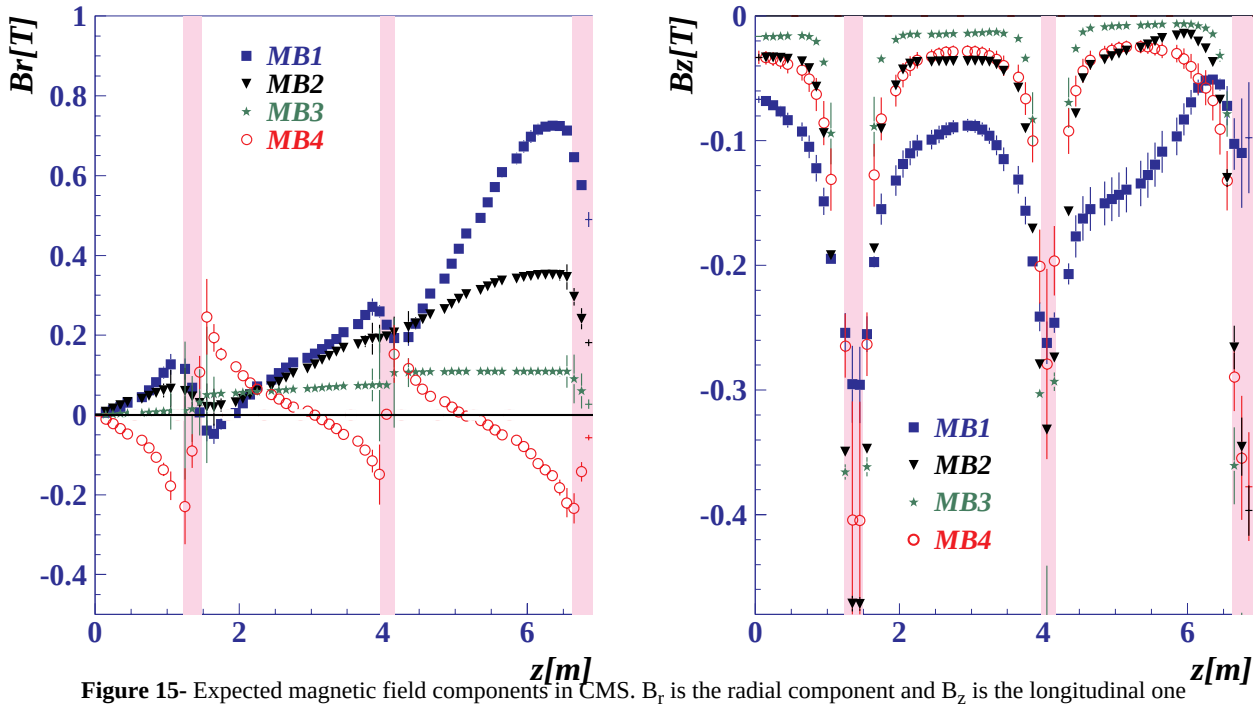

Figure 15- Expected magnetic field components in CMS. B_r is the radial component and B_z is the longitudinal one

5.2.1 Performance under B_w

The BTI efficiency for some track inclinations as a function of B_w is shown in Figure 16. The asymmetry in the performance is due to the fact the magnetic field distortion is compensating the existing non linearity for one sign of the angle, while it is worsening it for the opposite sign.

This effect was already observed [6] and was expected from previous analysis on the drift velocity apparent changes [2].

The relative fraction of HTRGs and LTRGs is reported in Figure 17: the efficiency drop is clearly accompanied by a degradation of the trigger quality. If, as expected, the B_w component on CMS will be below 0.2T the effect of line twirling due to this magnetic field component will be acceptable.

Of course the other observable effect is the increase of the HTRG noise. The fraction of out of time HTRGs is shown in Figure 18, while Figure 19 details this fraction for the steps just before (step -1) or just after (step +1) the right bunch crossing assignment.

5.2.2 Performance under B_E

The BTI efficiency in the presence of the B_E component only is shown in Figure 20: as expected the Lorentz force in null and no evident effect is seen.

5.2.3 Performance under mixed (B_n,B_E)

In this situation the field components were $B_n = B \sin\theta$ and $B_E = B \cos\theta$. The existence of a B_n component that is rotating the electron path by the Lorentz angle implies that even the Lorentz force due to the B_E component is not null. A first order approximation is that its effect is similar to a B_w component of the order of $B_E \sin \alpha_L$, where α_L is the corresponding Lorentz angle

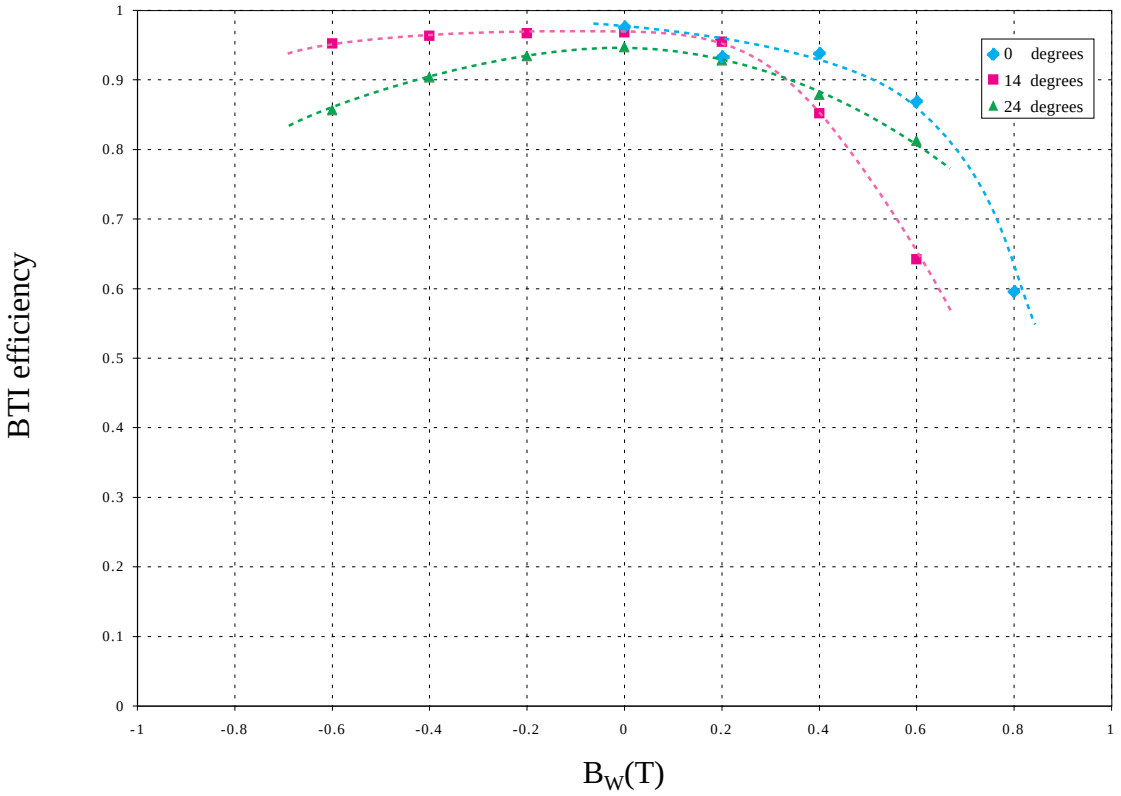

Figure 16- BTI efficiency as a function of B_w for several track inclinations without LTS.

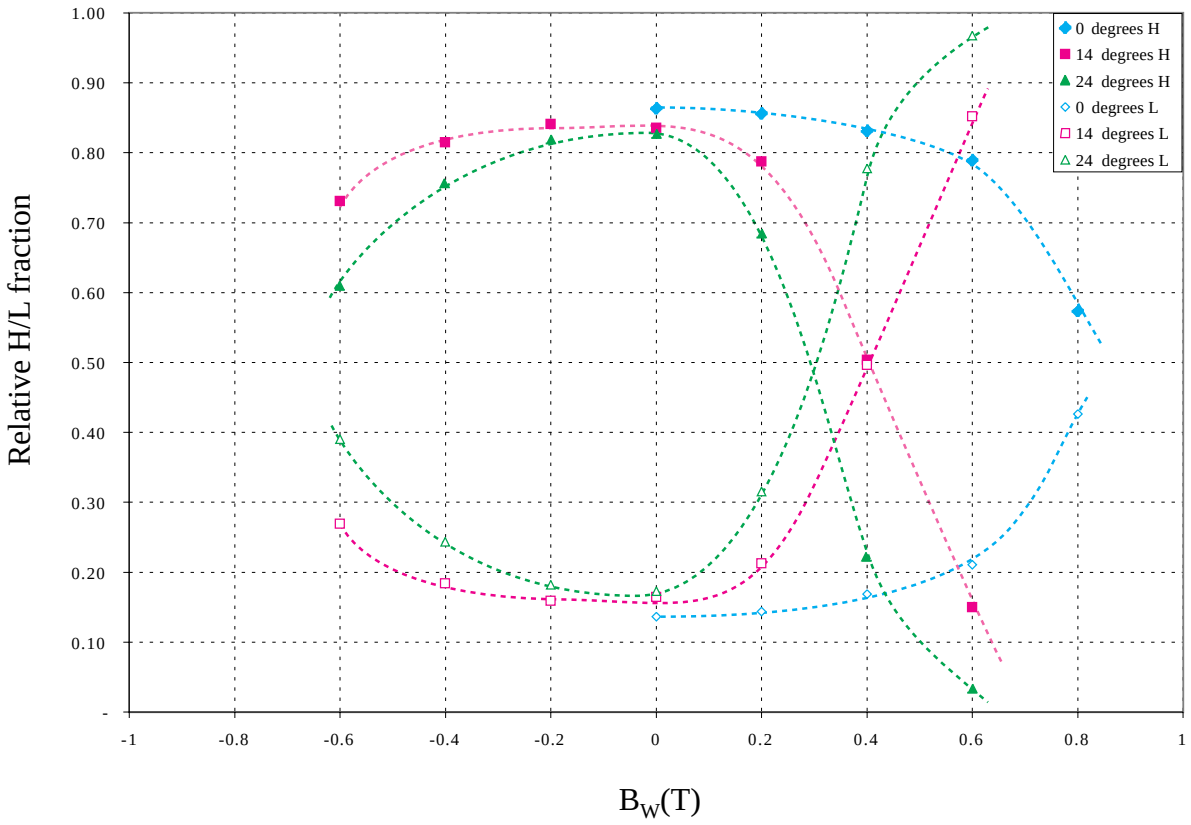

Figure 17- Relative fraction of HTRGs and LTRGs as a function of B_w for several track inclinations.

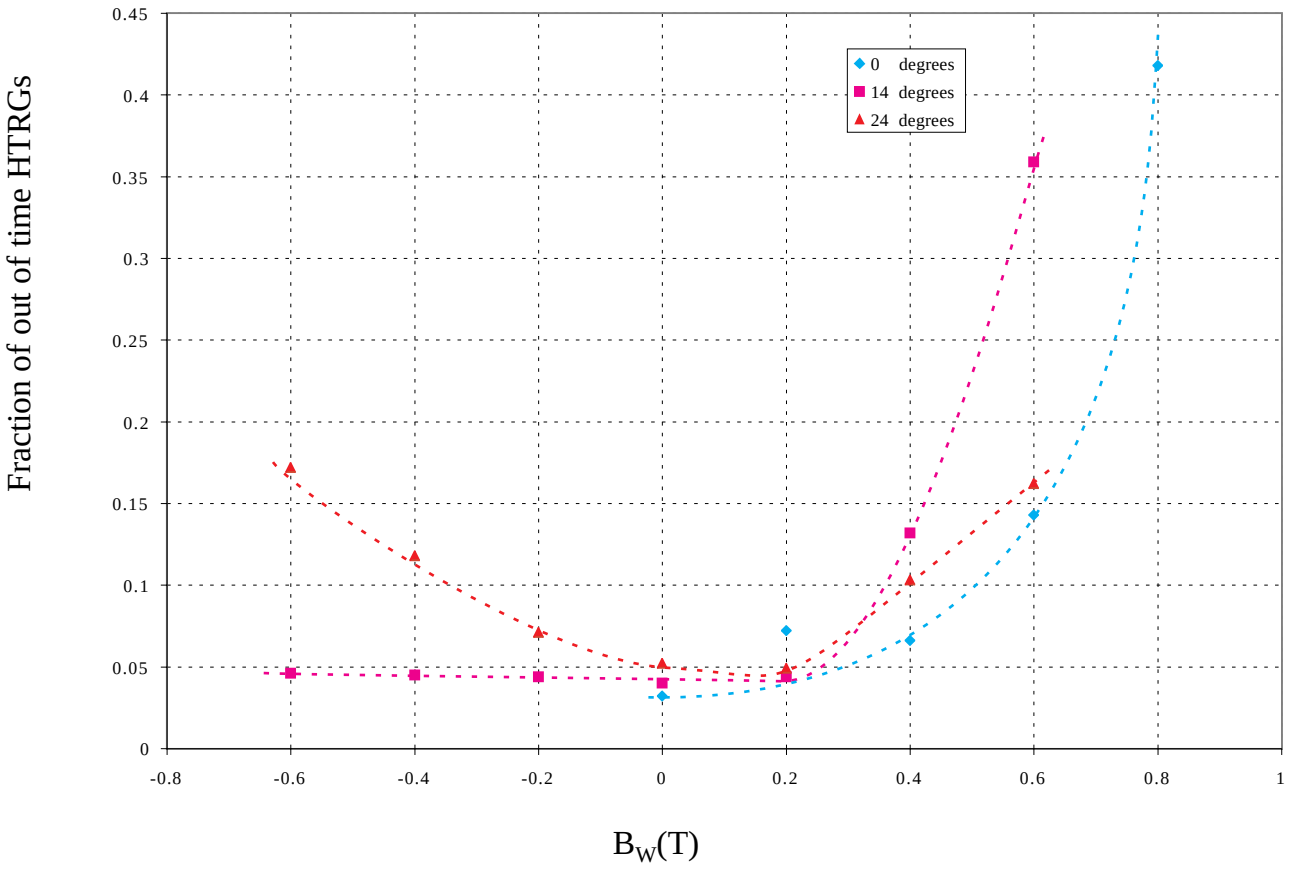

Figure 18- Fraction of out of time HTRGs as a function of B_w for several track inclinations.

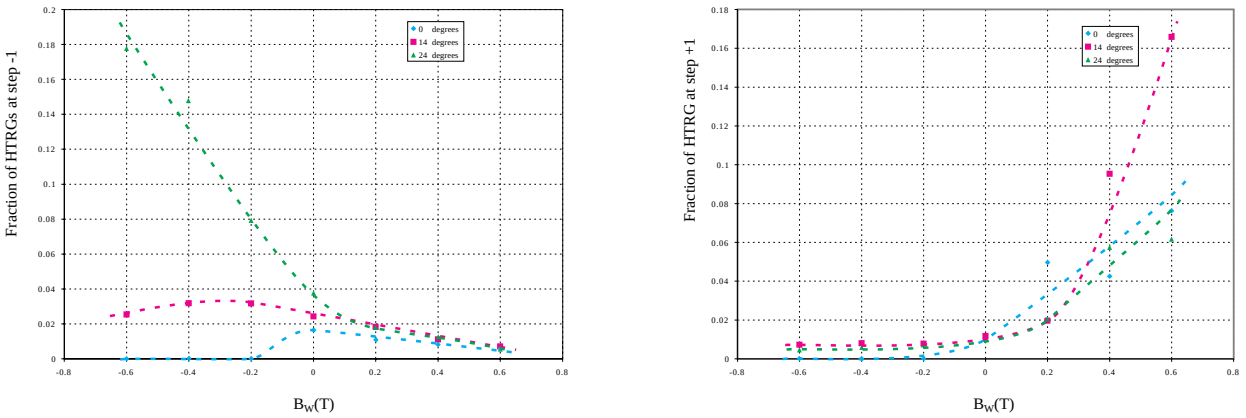

Figure 19- Fraction of out of time HTRGs as a function of B_w for several track inclinations at the steps nearby the right bunch crossing

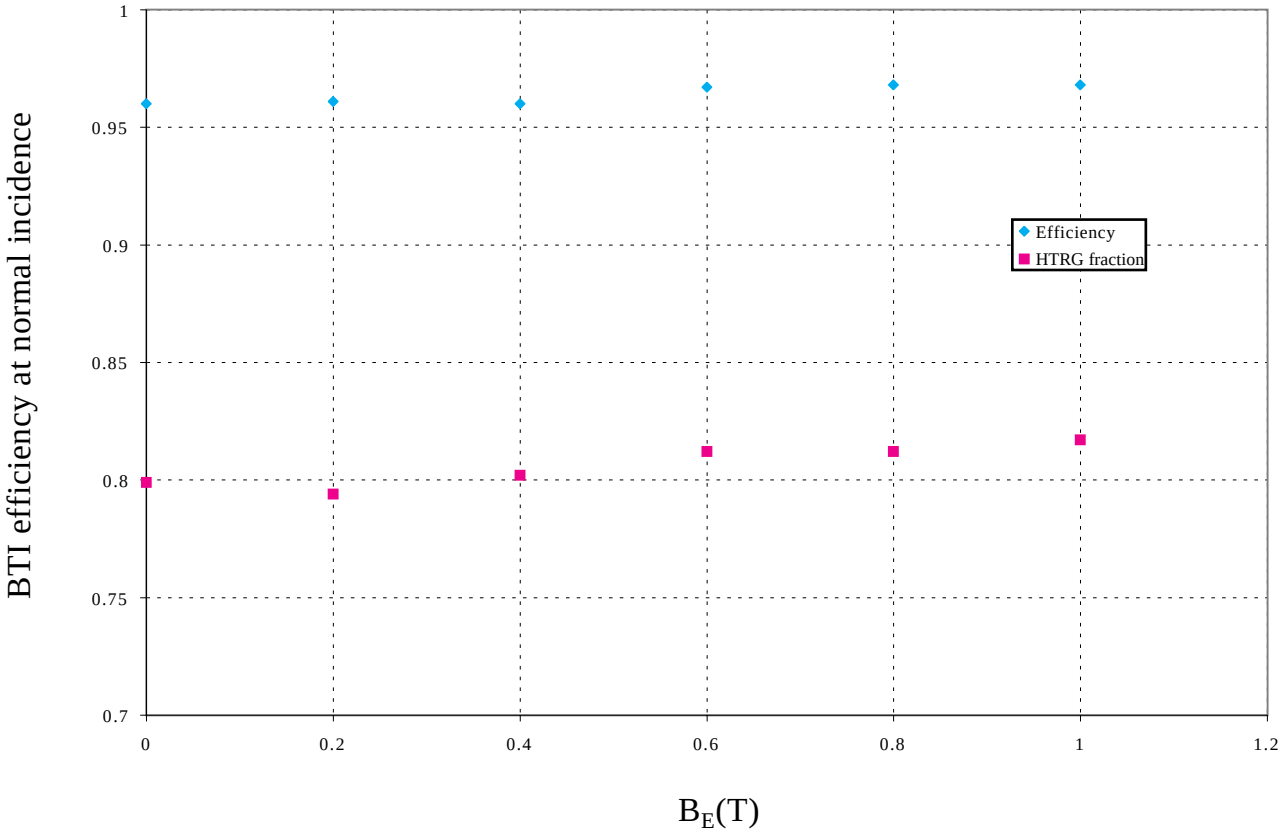

Figure 20- BTI efficiency as a function of the B_E component at normal incidence.

(at most B = 1T and α_L = 20° that holds an equivalent B_w of ~0.3T). The correlation between the non linearities introduced by B_n and the B_w equivalent twirling effect is unpredictable.

The efficiency versus the B_n component for the various chamber inclinations is shown in Figure 21. The existing B_E component can be determined at each measurement point with the formula $B_E = B_n / \tan \theta$.

It is difficult to separate effects related to incident angle, B_E component and B_n component, but the reasonably constant efficiency found for each chamber inclination supports the conclusion that the B_n magnetic field component has negligible effects up to B_n ~ 0.6T.

5.2.4 Performance under mixed (B_n,B_w)

In this situation the field components were $B_n = B \sin \theta$ and $B_w = B \cos \theta$. The presence of such a large B_w component implies that its effect is dominating the BTI performance as it can be deduced from Figure 22.

The test done with both components acting on the chamber extends to larger inclination angles the results already obtained with the tests performed only with the B_w component. We see that the chamber behaviour is still acceptable at 34°, but an important efficiency drop occurs at 40°.

The BTI is designed to have a flat response for tracks at incident angles till 45° and rapidly loses efficiency at larger angles [5]. Actually Figure 22 shows that an effect associated to B_w is the reduction of the response plateau below 40°.

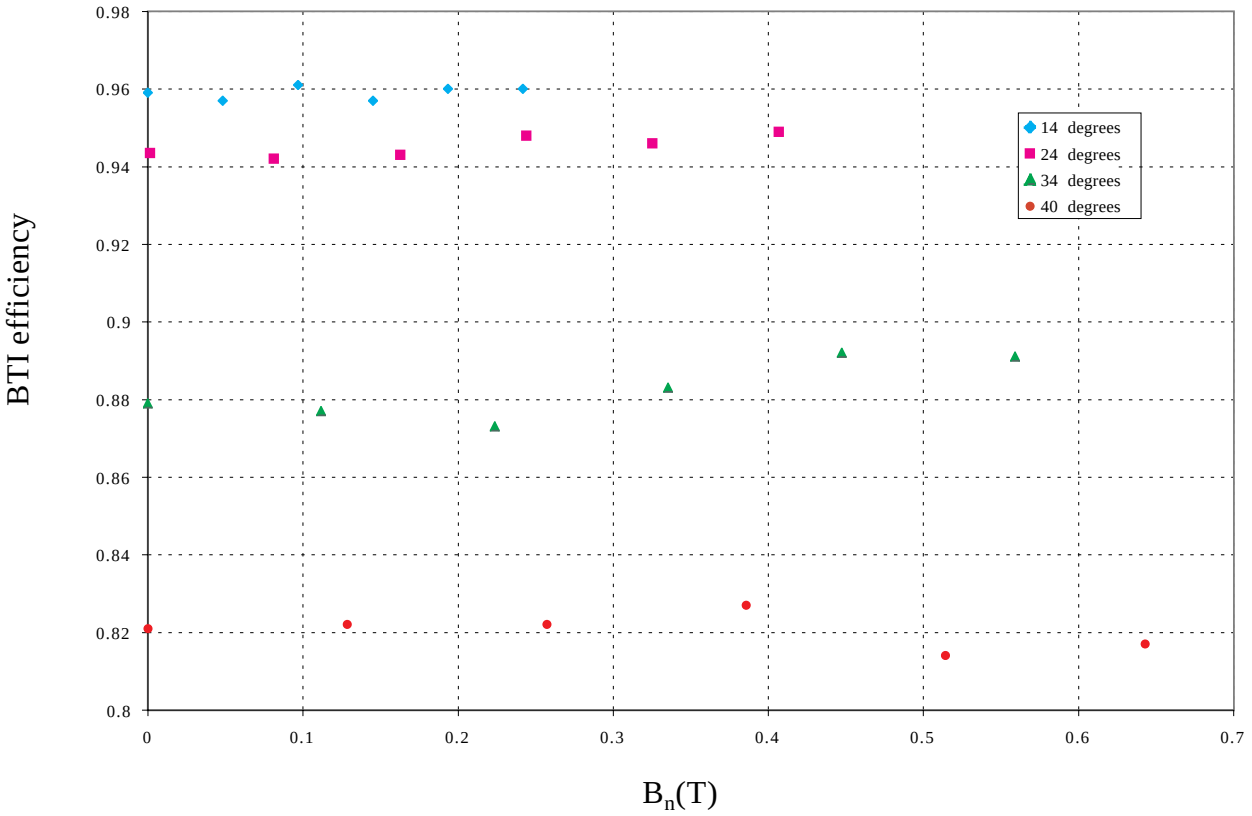

Figure 21- BTI efficiency as a function of B_n in presence of a B_E component.

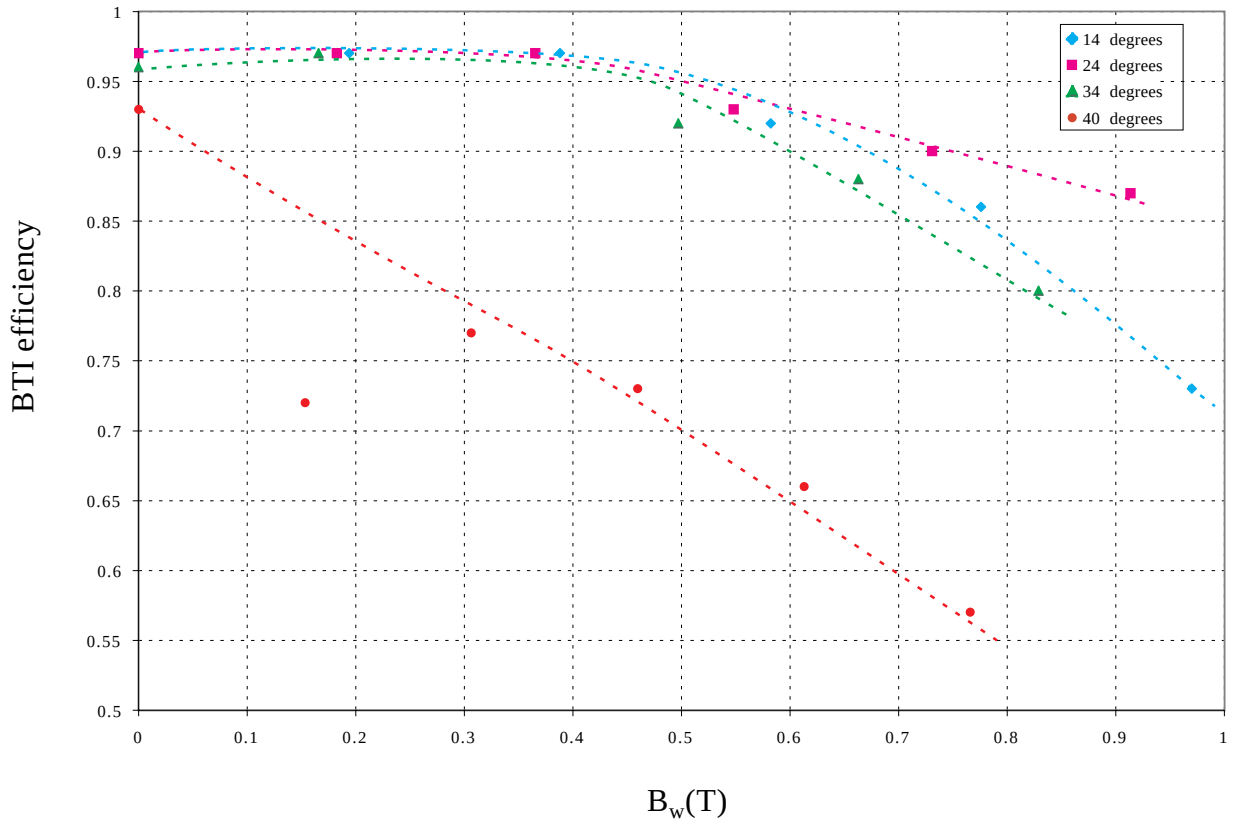

Figure 22- BTI efficiency as a function of B_w in presence of a B_n component.

It is instead useless checking the behaviour of the BTI versus the B_n component since according to the results obtained with mixed (B_n,B_E) field components its contribution would be negligible.

6 Conclusions

The analysis of the data using the BTI model was done on several data samples obtaining relevant information about its behaviour in presence of magnetic field.The experimental conditions were not quite similar to those that will be found inside CMS, but were probably worse than should be expected.

Therefore we can safely state the BTI offers acceptable performance in the expected environment, unless the actual stray field will be substantially different from calculated predictions. In particular unknown problems could arise from possible innaccuracies on the evaluation of the longitudinal stray field since the BTI efficiency is strongly dependent on it and asymmetry effect are found.

The results confirm previous tests and the expectations from the analysis of cell behaviour in magnetic field.

Further beam tests are needed to complete this investigation. In particular a clean B_n effect evaluation and tests with mixed field components where B_n is large and B_w or B_E are small.

References

[1] M. Benettoni et al., Nucl Instr. and Meth. A410 (1998) 133.

[2] M. Aguilar-Benitez et al., Nucl Instr. and Meth. A416 (1998) 243.

[3] M. De Giorgi et al., Nucl Instr. and Meth. A438 (1999) 302.

[4] J. Berdugo et al., CIEMAT report 833 (1997).

[5] L. Castellani et al., Proceedings of the Fourth Workshop on electronics for LHC experiments, CERN/LHCC/98-36, p. 285

[6] M. De Giorgi et al., Nucl Instr. and Meth. A398 (1997) 203.